EUROPEAN JOURNAL OF PURE AND APPLIED MATHEMATICS
2025, Vol. 18, Issue 4, Article Number 6267
ISSN 1307-5543 – ejpam.com
Published by New York Business Global

A Hybrid Approach for Approximating a Smoking Epidemic Model via Caputos Derivative, a Novel Integral Transform, and Artificial Neural Networks

Rachid Belgacem[1], Ahmed Bokhari[1], Abdelkader Benali[1], Ibrahim Alraddadi[2,*], Hijaz Ahmad[3], Waleed Mohammed Abdelfattah[4,5]

[1] *Laboratory of Mathematics and its Applications LMA, Hassiba Benbouali University of Chlef, Algeria*
[2] *Department of Mathematics, Faculty of Science, Islamic University of Madinah, Madinah, Saudi Arabia*
[3] *Near East University, Operational Research Center in Healthcare, Near East Boulevard, PC: 99138 Nicosia/Mersin 10, Turkey*
[4] *College of Engineering, University of Business and Technology, Jeddah 23435, Saudi Arabia*
[5] *Department of Engineering Mathematics and Physics, Faculty of Engineering, Zagazig University, P.O. 44519, Egypt*

Abstract. This work focuses on obtaining approximate analytical solutions for a fractional-order smoking epidemic model formulated with the Caputo derivative. The model divides the population into five compartmentspotential smokers, current smokers, occasional smokers, permanent smokers, and temporary quittersallowing the fractional framework to capture the long-term memory effects in smoking dynamics. Transition rates between these compartments are described by a set of parameters that reflect realistic behavioral changes. To solve the non linear fractional differential system efficiently, we propose a new hybrid computational strategy that combines the Junaid integral transform $\mathcal{T}_{\mathcal{NG}}$ with the Adomian Decomposition Method (ADM) and an Artificial Neural Network (ANN). The combined $\mathcal{T}_{\mathcal{NG}}$ADM stage ensures rapid convergence and accurate series solutions, while the ANN improves predictive performance by learning directly from the system dynamics. Numerical simulations validate the effectiveness and computational efficiency of the proposed approach, demonstrating its suitability for modelling memory-dependent epidemiological processes.

2020 Mathematics Subject Classifications: 92D30, 92D25, 26A33, 65R10, 65L05
Key Words and Phrases: Fractional smoking epidemic model, Caputo fractional derivative, Junaid transform, Adomian decomposition method

*Corresponding author.
DOI: https://doi.org/10.29020/nybg.ejpam.v18i4.6267

Email addresses: R.belgacem@univ-chlef.dz (R. Belgacem), bokhari.ahmed@ymail.com (A. Bokhari), benali4848@gmail.com (A. Benali), Ialraddadi@iu.edu.sa (I. Alraddadi), hijaz.ahmad@neu.edu.tr (H. Ahmad), w.abdelfattah@ubt.edu.sa (W. M. Abdelfattah)

1. Introduction

In recent years, integral transforms have emerged as powerful mathematical tools, attracting increasing attention from researchers across various scientific fields. Their effectiveness in solving a wide range of linear equations including ordinary and partial differential equations (ODEs and PDEs), integral equations, and fractional differential equations (FDEs) lies in their ability to convert complex differential problems into simpler algebraic forms. This transformation simplifies the solution process and accelerates computations. As a result, integral transforms have found widespread application across various disciplines, fostering the development of new methods and enhancing existing ones. However, the inversion of these transforms remains a critical step in obtaining the final solution.

Recent advancements in integral transforms have revolutionized the computation of PDEs, enabling both precise and approximate solutions [1]. Their inherent capability to map functions between different domains while preserving key properties ensures efficient and accurate outcomes, making them indispensable in applied mathematics. Moreover, combining integral transforms with other techniques can effectively tackle the nonlinear components of equations, leading to more efficient solutions and improved accuracy [2]. One such technique is the Adomian Decomposition Method (ADM)[3], which has proven highly effective for solving complex ODEs, PDEs, and FDEs [4].

Over the past two decades, a variety of integral Laplace-type transformations have been developed, including the Sumudu [5], Elzaki [6], Natural [7], Aboodh [8], Mohand [9], Sawi [10], Shehu [11–14], Kamal[15] and Jafari [16, 17] transformations. More recently, hybrid approaches involving neural networks and integral transforms have been explored to approximate solutions of complex fractional models.

The successful application of hybrid methodologies to various fractional models provides strong justification for our approach. For instance, the generalized exponential rational function method has demonstrated remarkable efficacy in obtaining optical soliton solutions for dual-mode time-fractional nonlinear Schrödinger equations [18], while innovative approaches have been developed for solving (2+1)-dimensional generalized KdV equations [19]. These hybrid analytical-numerical techniques have shown great potential for handling complex nonlinear systems similar to our smoking epidemic model.

Similarly, the integration of neural networks with fractional calculus has emerged as a powerful paradigm. Recent work on modeling and neural network approximation of asymptotic behavior for delta fractional difference equations with Mittag-Leffler kernels [20] demonstrates how machine learning can enhance traditional analytical methods. This aligns with our approach of combining the $\mathcal{T}_{\mathcal{NG}}$-transform with artificial neural networks to improve accuracy and computational efficiency.

Our methodology also draws inspiration from finite difference approaches for fractional models [21] and analytical algebraic methods for nonlinear fractional differential equations [22]. These established techniques provide a solid foundation for our hybrid $\mathcal{T}_{\mathcal{NG}}$-ADM-ANN framework, adapting proven methods to the specific challenges of smoking epidemic modelling.

In the reference [23], the author proposed a new generalized integral transform, which

will be referred to as such $\mathcal{T}_{\mathcal{NG}}$-transform throughout this paper. This transform was used in conjunction with the ADM method to solve non-linear PDEs, including the gas dynamic equation and the system of coupled Burgers' equations.

Motivation and Originality

This work makes several original contributions that advance both the theoretical and computational treatment of FDEs. First, we present the explicit derivation of the specific integral transform $\mathcal{T}_{\mathcal{NG}}$ for the CF derivative, establishing a rigorous analytical framework that enables the systematic conversion of FDEs into an equivalent algebraic form. We further prove several recent results regarding its operational properties, which significantly enrich the transform's analytical capabilities. Second, we develop a new hybrid technique, denoted as $\mathcal{T}_{\mathcal{NG}}$-ADM, which synergistically combines the $\mathcal{T}_{\mathcal{NG}}$-transform with the ADM method. This approach produces series solutions with rapid convergence and incorporates auxiliary parameters to fine-tune and optimize the convergence process. Finally, we integrate an artificial neural network (ANN) algorithm to enhance the approximation accuracy for the fractional smoking epidemic model, significantly improving the robustness, precision, and applicability of the proposed methodology to real-world problems.

The novelty of our work lies in the unique combination of these established techniquesintegral transforms, decomposition methods, and neural networksspecifically adapted for Caputo fractional-order epidemiological models. While each component has been individually validated in previous studies, their integration into a unified framework for smoking dynamics represents a significant advancement in computational epidemiology [24, 25].

This manuscript is structured as follows. Section 2 reviews the fundamental concepts of fractional calculus and the essential properties of the proposed general integral transform ($\mathcal{T}_{\mathcal{NG}}$). Section 3 presents the main theoretical results of the $\mathcal{T}_{\mathcal{NG}}$ transform, including explicit formulations for the Caputo fractional derivative (CFD), the RiemannLiouville fractional derivative (RLFD), and the RL fractional integral (RLFI), along with its key operational properties. Section 4 addresses the mathematical modelling of the fractional smoking epidemic model and highlights its principal analytical properties. Sections 5 and 6 present a hybrid $\mathcal{T}_{\mathcal{NG}}$-ADM method for solving the fractional model, further enhanced by integration with an ANN to improve accuracy and robustness. Finally, the study highlights the method's advantages and outlines directions for future work.

2. Preliminary

This first section presents fundamental definitions in fractional calculus and highlights key properties of the Junaid transform, which will serve as the basis for the analyses that follow.

Definition 1. *For a given function $\mathcal{V}(t)$, the RLFI of order $\alpha > 0$, is defined as [26]:*

$$ {}^{RL}I^{\alpha}_{0,t}\mathcal{V}(t) = \frac{1}{\Gamma(\alpha)}\int_0^t \frac{\mathcal{V}(\tau)}{(t-\tau)^{1-\alpha}}\,d\tau = \frac{1}{\Gamma(\alpha)}\,t^{\alpha-1}\star\mathcal{V}(t), \quad t>0. \tag{1}$$

The RLFD of order $\alpha > 0$, is given by:

$$ {}^{RL}D^{\alpha}_{0,t}\mathcal{V}(t) = \frac{d^m}{dt^m}\left({}^{RL}I^{m-\alpha}_{0,t}\mathcal{V}(t)\right) = \frac{d^m}{dt^m}\int_0^t \frac{\mathcal{V}(x)}{\Gamma(m-\alpha)(t-x)^{m-\alpha-1}}\,dx, \tag{2} $$

where $m-1<\alpha\le m$, $m\in\mathbb{N}$, and $\Gamma(.)$ denotes the Gamma function.

Definition 2. *For a given function $\mathcal{V}(t)$, the CFD of order $\alpha>0$, is described as: [27]:*

$$ \begin{aligned} {}^{C}D^{\alpha}_{0,t}\mathcal{V}(t) &= \frac{1}{\Gamma(m-\alpha)}\int_a^t \frac{\mathcal{V}^{(m)}(\tau)\,d\tau}{(t-\tau)^{1-m+\alpha}}, \quad 0<m-1<\alpha<m, m\in\mathbb{N}, \\ &= \frac{d^m}{t^m}v(t), \quad \alpha=m. \end{aligned} \tag{3} $$

Lemma 1. *If $\mathcal{V}\in AC^m[a,b]$ or $\mathcal{V}(t)\in C^m[a,b]$, then [26]:*

$$ \left({}^{RL}I^{\alpha}_{0,t}\,{}^{C}D^{\alpha}_{0,t}\right)\mathcal{V}(t) = \mathcal{V}(t) - \sum_{k=0}^{m-1}\frac{\mathcal{V}^{(k)}(0)}{k!}t^k, \tag{4} $$

where $m=[\alpha]+1$ and $[\alpha]$ represents the integer part of arbitrary $\alpha>0$.

The Junaid integral transform of the integrable function $\mathcal{V}(t)$ was recently introduced by Junaid [23] in 2023, by

$$ \mathcal{T}_{\mathcal{NG}}[\mathcal{V}(t)] = \mathcal{M}(s)\int_0^{\infty}\mathcal{V}(\mathcal{K}(s)t)\exp^{-\mathcal{B}(s)t}\,dt, \tag{5} $$

where $\mathcal{M}(s),\mathcal{B}(s)$ and $\mathcal{K}(s)$ are positive real functions and $t\ge 0$ such that $\mathcal{M}(s)\neq 0$.

This $\mathcal{T}_{\mathcal{NG}}$ transform can be easily implemented directly to an appropriate problem by specifically selecting $\mathcal{M}(s)$, $\mathcal{B}(s)$ and $\mathcal{K}(s)$. In Table 1, we mention the $\mathcal{T}_{\mathcal{NG}}$ transform of some basic function.

$\mathcal{V}(t)$	$\mathcal{T}_{\mathcal{NG}}[\mathcal{V}(t)]$
c	$c\dfrac{\mathcal{M}(s)}{\mathcal{B}(s)}, \quad c\in\mathbb{R}$
t	$\dfrac{\mathcal{M}(s)\mathcal{K}(s)}{\mathcal{B}^2(s)}$
t^n	$\dfrac{n!\mathcal{M}(s)r^n(s)}{\mathcal{B}^{n+1}(s)}$
$\sin t$	$\dfrac{\mathcal{M}(s)\mathcal{K}(s)}{\mathcal{B}^2(s)+r^2(s)}$
e^t	$\dfrac{\mathcal{M}(s)}{\mathcal{B}(s)-\mathcal{K}(s)}$

Table 1: $\mathcal{T}_{\mathcal{NG}}$ transform for some basic functions.

Theorem 1. *The $\mathcal{T}_{\mathcal{NG}}$ transform of n^{th} derivative $\mathcal{V}^{(n)}(t)$ of the function $\mathcal{V}(t)$, is expressed as [23]:*

$$\mathcal{T}_{\mathcal{NG}}\left[\mathcal{V}^{(n)}(t)\right]=\left(\frac{\mathcal{B}(s)}{\mathcal{K}(s)}\right)^{n}\mathcal{T}_{\mathcal{NG}}\left[\mathcal{V}(t)\right]-\mathcal{M}(s)\sum_{i=0}^{n-1}\frac{\mathcal{B}^{n-1-i}(s)}{\mathcal{K}^{n-i}(s)}\mathcal{V}^{(i)}(0),\forall n\in\mathbb{N}. \tag{6}$$

The next section presents new results about this generalization transform, as a complement to the results presented in [23].

3. Main results of $\mathcal{T}_{\mathcal{NG}}$ transform

Property 1. *(Convolution) Let $\mathcal{T}_{\mathcal{NG}}[\mathcal{V}_1(t)]$ and $\mathcal{T}_{\mathcal{NG}}[\mathcal{V}_2(t)]$ are $\mathcal{T}_{\mathcal{NG}}$ transforms of $\mathcal{V}_1(t)$ and $\mathcal{V}_2(t)$, respectively. Then:*

$$\mathcal{T}_{\mathcal{NG}}\left[\mathcal{V}_1\star\mathcal{V}_2\right]=\int_0^{\infty}\mathcal{V}_1(t)\,\mathcal{V}_2(t-z)\,dz=\frac{\mathcal{K}(s)}{\mathcal{M}(s)}\mathcal{T}_{\mathcal{NG}}\left[\mathcal{V}_1(t)\right]\mathcal{T}_{\mathcal{NG}}\left[\mathcal{V}_2(t)\right]. \tag{7}$$

Proof. We have:

$$\mathcal{V}_1\star\mathcal{V}_2=\int_0^{\infty}\mathcal{V}_1(z)\,\mathcal{V}_2(t-z)\,dz,$$

using the $\mathcal{T}_{\mathcal{NG}}$ transform and the Leibniz theorem, we get:

$$\begin{aligned}\mathcal{T}_{\mathcal{NG}}\left[\mathcal{V}_1\star\mathcal{V}_2\right]&=\mathcal{T}_{\mathcal{NG}}\left[\int_0^{\infty}\mathcal{V}_1(z)\,\mathcal{V}_2(t-z)\,dz\right],\\&=\mathcal{M}(s)\int_0^{\infty}\left[\int_0^{\infty}\mathcal{V}_1(\mathcal{K}(s)\,z)\,\mathcal{V}_2(\mathcal{K}(s)\,(t-z))\,\mathcal{K}(s)\,dz\right]\exp^{-\mathcal{B}(s)t}\,dt,\\&=\mathcal{M}(s)\,\mathcal{K}(s)\int_0^{\infty}\mathcal{V}_1(\mathcal{K}(s)\,z)\left[\int_0^{\infty}\mathcal{V}_2(\mathcal{K}(s)\,(t-z))\exp^{-\mathcal{B}(s)t}\,dt\right]dz.\end{aligned}$$

By setting $\tau=t-z$, we get:

$$\begin{aligned}\mathcal{T}_{\mathcal{NG}}\left[\mathcal{V}_1\star\mathcal{V}_2\right]&=\mathcal{M}(s)\,\mathcal{K}(s)\int_0^{\infty}\mathcal{V}_1(\mathcal{K}(s)\,z)\left[\int_0^{\infty}\mathcal{V}_2(\tau)\exp^{-\mathcal{B}(s)(\tau+z)}\,d\tau\right]dz,\\&=\frac{\mathcal{K}(s)}{\mathcal{M}(s)}\left[\mathcal{M}(s)\int_0^{\infty}\mathcal{V}_1(\mathcal{K}(s)\,z)\exp^{-\mathcal{B}(s)z}\,dz\right]\left[\mathcal{M}(s)\int_0^{\infty}\mathcal{V}_2(\tau)\exp^{-\mathcal{B}(s)\tau}\,d\tau\right],\\&=\frac{\mathcal{K}(s)}{\mathcal{M}(s)}\mathcal{T}_{\mathcal{NG}}\left[\mathcal{V}_1(t)\right]\mathcal{T}_{\mathcal{NG}}\left[\mathcal{V}_2(t)\right].\end{aligned}$$

Property 2. *When $\mathcal{V}(t)=t^{x-1}$ in formula of $\mathcal{T}_{\mathcal{NG}}$ transform 5, then:*

$$\mathcal{T}_{\mathcal{NG}}\left[t^{x-1}\right]=\frac{\Gamma(x)\,\mathcal{M}(s)\,\mathcal{K}^{x-1}(s)}{\mathcal{B}^{x}(s)}. \tag{8}$$

Proof. From the formula 5, we obtain:

$$\begin{aligned}\mathcal{T}_{\mathcal{NG}}\left[t^{x-1}\right] &= \mathcal{M}(s)\int_0^{\infty}(\mathcal{K}(s)t)^{x-1}\exp^{-\mathcal{B}(s)t}dt,\\ &= \mathcal{M}(s)\mathcal{K}^{x-1}(s)\int_0^{\infty}t^{x-1}\exp^{-\mathcal{B}(s)t}dt.\end{aligned}$$

If we set $\xi = \mathcal{B}(s)t\left(t=\dfrac{\xi}{\mathcal{B}(s)}\right)$, then

$$\begin{aligned}\mathcal{T}_{\mathcal{NG}}\left[t^{x-1}\right] &= \frac{\mathcal{M}(s)\mathcal{K}^{x-1}(s)}{\mathcal{B}^{x}(s)}\int_0^{\infty}\xi^{x-1}\exp^{-\xi}d\xi,\\ &= \frac{\mathcal{M}(s)\mathcal{K}^{x-1}(s)}{\mathcal{B}^{x}(s)}\Gamma(x).\end{aligned}$$

Lemma 2. *The $\mathcal{T}_{\mathcal{NG}}$ transform of the fractional integral ${}^{RL}I_{0,t}^{\alpha}$ of $\mathcal{V}$, is formulated as:*

$$\mathcal{T}_{\mathcal{NG}}\left[\left({}^{RL}I_0^{\alpha}\mathcal{V}\right)(t)\right] = \frac{\mathcal{K}^{\alpha}(s)}{\mathcal{B}^{\alpha}(s)}\mathcal{T}_{\mathcal{NG}}\left[\mathcal{V}(t)\right]. \tag{9}$$

Proof.
Applying $\mathcal{T}_{\mathcal{NG}}$ transform and according to properties 1 and 2, we have:

$$\begin{aligned}\mathcal{T}_{\mathcal{NG}}\left[{}^{RL}I_{0,t}^{\alpha}\mathcal{V}(t)\right] &= \mathcal{T}_{\mathcal{NG}}\left[\frac{1}{\Gamma(\alpha)}t^{\alpha-1}\star\mathcal{V}(t)\right],\\ &= \frac{\mathcal{K}(s)}{\mathcal{M}(s)}\frac{\mathcal{M}(s)r^{\alpha-1}(s)}{\mathcal{B}^{\alpha}(s)}\mathcal{T}_{\mathcal{NG}}\left[\mathcal{V}(t)\right],\\ &= \frac{\mathcal{K}^{\alpha}(s)}{\mathcal{B}^{\alpha}(s)}\mathcal{T}_{\mathcal{NG}}\left[\mathcal{V}(t)\right].\end{aligned}$$

Lemma 3. *The $\mathcal{T}_{\mathcal{NG}}$ transform of the ${}^{RL}D_0^{\alpha}$ of $\mathcal{V}$, is given as follows:*

$$\mathcal{T}_{\mathcal{NG}}\left\{{}^{RL}D_{0,t}^{\alpha}\mathcal{V}(t),s\right\} = \left(\frac{\mathcal{B}(s)}{\mathcal{K}(s)}\right)^{\alpha}\mathcal{T}_{\mathcal{NG}}\left[\mathcal{V}(t)\right] - \mathcal{M}(s)\sum_{k=0}^{m-1}\frac{\mathcal{B}^{m-1-k}(s)}{\mathcal{K}^{m-k}(s)}\left[{}^{RL}D_{0,t}^{\alpha-k-m}\mathcal{V}(t)\right]_{t=0}, \tag{10}$$

where $m-1<\alpha\leq m$.

Proof. Applying the $\mathcal{T}_{\mathcal{NG}}$ transform to both sides of equation (2), followed by the use of Lemma (2) and Theorem (1), yields:

$$\mathcal{T}_{\mathcal{NG}}\left[{}^{RL}D_{0,t}^{\alpha}\mathcal{V}(t)\right] = \mathcal{T}_{\mathcal{NG}}\left[\frac{d^m}{dt^m}I_{0,t}^{m-\alpha}\mathcal{V}(t)\right],$$

$$= \left(\frac{\mathcal{B}(s)}{\mathcal{K}(s)}\right)^{m} \mathcal{T}_{\mathcal{NG}}\left[I_{0,t}^{m-\alpha}\mathcal{V}(t)\right] - \mathcal{M}(s)\sum_{k=0}^{m-1}\frac{\mathcal{B}^{m-1-k}(s)}{\mathcal{K}^{m-k}(s)}\left[\left(\frac{d}{dt}\right)^{(k)} I_{0,t}^{m-\alpha}\mathcal{V}(t)\right]_{t=0},$$

$$= \left(\frac{\mathcal{B}(s)}{\mathcal{K}(s)}\right)^{\alpha} \mathcal{T}_{\mathcal{NG}}\left[\mathcal{V}(t)\right] - \mathcal{M}(s)\sum_{k=0}^{m-1}\frac{\mathcal{B}^{m-1-k}(s)}{\mathcal{K}^{m-k}(s)}\left[{}^{RL}D_{0,t}^{\alpha-k-m}\mathcal{V}(t)\right]_{t=0}.$$

Hence, the desired result (10) is established.

Theorem 2. *If $\mathcal{V} \in AC^m(a,b)$ for any $b > a$ and of exponential order. Then, the $\mathcal{T}_{\mathcal{NG}}$ transform of the ${}^{C}D_0^{\alpha}$ of $\mathcal{V}$ is given by:*

$$\mathcal{T}_{\mathcal{NG}}\left[{}^{C}D_0^{\alpha}\mathcal{V}(t)\right] = \frac{\mathcal{B}^{\alpha}(s)}{\mathcal{K}^{\alpha}(s)}\mathcal{T}_{\mathcal{NG}}\left[\mathcal{V}(t)\right] - \sum_{k=0}^{m-1}\frac{\mathcal{M}(s)\mathcal{B}^{\alpha-k-1}(s)}{\mathcal{K}^{\alpha-k}(s)}\mathcal{V}^{(k)}(0). \tag{11}$$

Proof. Since $\left({}^{RL}I_{0,t}^{\alpha}\,{}^{C}D_{0,t}^{\alpha}\right)\mathcal{V}(t) = \mathcal{V}(t) - \sum_{k=0}^{m-1}\frac{\mathcal{V}^{(k)}(0)}{k!}t^k$. According to Lemma 1, we have:

$$\mathcal{T}_{\mathcal{NG}}\left[\left({}^{RL}I_{0,t}^{\alpha}\,{}^{C}D_{0,t}^{\alpha}\right)\mathcal{V}(t)\right] = \mathcal{T}_{\mathcal{NG}}\left[\mathcal{V}(t) - \sum_{k=0}^{m-1}\frac{\mathcal{V}^{(k)}(0)}{k!}t^k\right], \tag{12}$$

therefore, the Eq 12 becomes,

$$\frac{\mathcal{K}^{\alpha}(s)}{\mathcal{B}^{\alpha}(s)}\mathcal{T}_{\mathcal{NG}}\left[{}^{C}D_0^{\alpha}\mathcal{V}(t)\right] = \mathcal{T}_{\mathcal{NG}}\left[\mathcal{V}(t)\right] - \sum_{k=0}^{m-1}\frac{\mathcal{V}^{(k)}(0)}{k!}\frac{k!\mathcal{M}(s)\mathcal{K}^{k}(s)}{\mathcal{B}^{k+1}(s)}.$$

Finally, we obtain:

$$\mathcal{T}_{\mathcal{NG}}\left[{}^{C}D_{0,t}^{\alpha}\mathcal{V}(t)\right] = \frac{\mathcal{B}^{\alpha}(s)}{\mathcal{K}^{\alpha}(s)}\mathcal{T}_{\mathcal{NG}}\left[\mathcal{V}(t)\right] - \sum_{k=0}^{m-1}\frac{\mathcal{M}(s)\mathcal{B}^{\alpha-k-1}(s)}{\mathcal{K}^{\alpha-k}(s)}\mathcal{V}^{(k)}(0).$$

This concludes the proof.

4. Main results and Mathematical Modeling of Smoking epidemic Model

Many mathematical models are employed to grasp biological phenomena through an examination of their dynamic behavior. In our research, we consider a system comprising five non linear FDEs that characterize the smoking epidemic model, incorporating the ${}^{C}D_{0,t}^{\alpha}$, where $0 < \alpha < 1$. This model is formulated in [28] as follows:

$$\begin{cases} {}^{C}D_{0,t}^{\alpha}(P(t)) = \lambda - \beta P(t)S(t) - \mu P(t), \\ {}^{C}D_{0,t}^{\alpha}(O(t)) = \beta P(t)S(t) - \alpha_1 O(t) - \mu O(t), \\ {}^{C}D_{0,t}^{\alpha}(S(t)) = \alpha_1 O(t) + \alpha_2 S(t)Q(t) - (\mu+\gamma)S(t), \\ {}^{C}D_{0,t}^{\alpha}(Q(t)) = -\alpha_2 S(t)Q(t) - \mu Q(t) + \gamma(1-\delta)S(t), \\ {}^{C}D_{0,t}^{\alpha}(L(t)) = \delta\gamma S(t) - \mu L(t), \end{cases} \tag{13}$$

subject to the following initial conditions

$$P(0) = b_1, O(0) = b_2, S(0) = b_3, Q(0) = b_4, L(0) = b_5. \tag{14}$$

The behavior of the model dynamics under various parameter settings is illustrated in Figure 1.

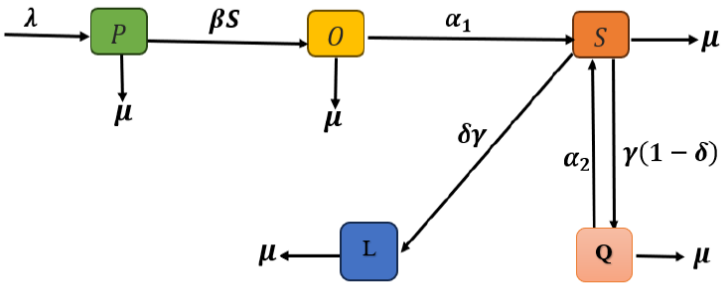

Figure 1: A graphical illustration of the envisaged mathematical model concerning the smoking epidemic

For $\alpha = 1$, the system reduces to ordinary differential equations. In this model 13, we divide the total population size at time t denoted by $N(t)$ into five subgroups: potential smokers represented by $P(t)$, current smokers denoted as $S(t)$, occasional smokers labeled $O(t)$, individuals who have permanently quit smoking indicated by $L(t)$, and those who have temporarily quit smoking represented by $Q(t)$.The parameters used in model 13, along with their detailed descriptions, are listed in Table 2 below.

Table 2: Parameters used in the model and their descriptions.

Parameter	**Description**
λ	Recruitment rate in population P
β	Effective contact rate between S and P
μ	Natural death rate
α_1	Rate at which occasional smokers convert to regular smokers
α_2	Contact rate between smokers and temporary quitters who revert back to smoking
γ	Rate of quitting smoking
$1-\delta$	Fraction of smokers who temporarily quit smoking (at rate γ)
δ	Fraction of smokers who permanently quit smoking

Lemma 4. *When $\alpha = 1$ in system (13), all possible solutions are bounded and confined within the region defined by:*

$$\Omega = \left\{ (P,O,S,Q,L) \in \mathbb{R}^5_+ : P+O+S+Q+L \leqslant \frac{\lambda}{\mu} \right\}. \tag{15}$$

Proof. Let $(P,O,S,Q,L) \in \mathbb{R}^5_+$ be any solution with not negative subject to initial conditions, then:

$$\frac{dN(t)}{d(t)} = \lambda - \mu N(t),$$

Consequently,

$$0 \leqslant N(t) \leqslant \frac{\lambda}{\mu} + N(0)e^{-\mu t},$$

where $N(0)$ represents the initial value of $N(t)$. Thus,

$$0 \leqslant N(t) \leqslant \frac{\lambda}{\mu} \quad \text{as} \quad t \to \infty.$$

Therefore, all possible solutions of the system lie within the region Ω. Hence, Ω is positively invariant.

Combining the equations from the (13), and considering the linearity of ${}^{C}D^{\alpha}_{0,t}$, we derive:

$${}^{C}D^{\alpha}_{0,t}(N(t)) = \lambda - \mu N(t). \tag{16}$$

When the initial conditions for the model (13) are positive, it has a unique positive solution (see the work of [28]). We also address in the following that system (13) has two equilibrium, the Smoking-Free Equilibrium (SFE) and the Smoking-Present Equilibrium (SPE). Then, the local and global stability results of the equilibrium are also obtained. First, employing the next-generation matrix method as formulated in [**?**], we analyze the existence of the point (SFE), Let $\mathcal{Y} = (O,S,Q,L,P)^T$, whereby the model can be expressed as:

$${}^{C}D^{\alpha}_{0,t}(\mathcal{Y}) = \mathcal{F}(\mathcal{Y}) + \mathcal{H}(\mathcal{Y}), \tag{17}$$

where

$$\mathcal{F}(\mathcal{Y}) = \begin{pmatrix} \beta P(t)S(t) \\ 0 \\ 0 \\ 0 \\ 0 \end{pmatrix}, \tag{18}$$

and

$$\mathcal{H}(\mathcal{Y}) = \begin{pmatrix} -(\alpha_1 + \mu)O \\ \alpha_1 O + \alpha_2 SQ - (\mu + \gamma)S \\ -\alpha_2 SQ - \mu Q + \gamma - \delta\gamma S \\ \delta\gamma S - \mu L \\ \lambda - \beta PS - \mu P \end{pmatrix}. \tag{19}$$

By replacing $S = 0$ in (13), we obtian the following result.

Proposition 1. *For the our model (13), an SEP exists, denoted by E_0, with $E_0 = (\frac{\lambda}{\mu}, 0, 0, 0, 0)$.*

Proposition 2. *The Reproduction Number, $\mathcal{R}_0$, is determined as:*

$$\mathcal{R}_0 = \rho(-FV^{-1}) = \frac{\alpha_1 \beta P_0}{(\mu+\gamma)(\mu+\alpha_1)}, \tag{20}$$

where:

$$F = D\mathcal{F}(E_0) = \left(\begin{array}{ccc|cc} 0 & 0 & \beta P_0 & 0 & 0 \\ 0 & 0 & 0 & 0 & 0 \\ 0 & 0 & 0 & 0 & 0 \\ \hline 0 & 0 & 0 & 0 & 0 \\ 0 & 0 & 0 & 0 & 0 \end{array}\right), \tag{21}$$

$$V = D\mathcal{H}(E_0) = \left(\begin{array}{ccc|cc} 0 & -(\alpha_1+\mu) & 0 & 0 & 0 \\ 0 & \alpha_1 & -(\mu+\gamma) & 0 & 0 \\ 0 & 0 & \gamma(1-\delta) & -\mu & 0 \\ \hline 0 & 0 & \gamma\delta & 0 & -\mu \\ -\mu & 0 & -\beta P_0 & 0 & 0 \end{array}\right). \tag{22}$$

Here, $D\mathcal{H}(E_0)$ and $D\mathcal{F}(E_0)$ denote the Jacobian matrices of $\mathcal{H}(\mathcal{Y})$ and $\mathcal{F}(\mathcal{Y})$ evaluated at E_0 respectively.

Proof. A simple calculation gives: 21 and 22 (see [**?**]). So,

$$V = D\mathcal{V}(E_0) = \begin{pmatrix} -\alpha_1-\mu & 0 & 0 \\ \alpha_1 & -\mu-\gamma & 0 \\ 0 & \gamma-\gamma\delta & -\mu \end{pmatrix}, \; F = D\mathcal{F}(E_0) = \begin{pmatrix} 0 & \beta P_0 & 0 \\ 0 & 0 & 0 \\ 0 & 0 & 0 \end{pmatrix},$$

$$V^{-1} = \begin{pmatrix} -\frac{1}{\mu+\alpha_1} & 0 & 0 \\ -\frac{\alpha_1}{(\mu+\gamma)(\mu+\alpha_1)} & -\frac{1}{(\mu+\gamma)} & 0 \\ -\frac{\alpha_1\gamma(1-\delta)}{\mu(\mu+\gamma)(\mu+\alpha_1)} & -\frac{\gamma(1-\delta)}{\mu(\mu+\gamma)} & -\frac{1}{\mu} \end{pmatrix},$$

and

$$-FV^{-1} = \begin{pmatrix} \frac{\alpha_1\beta P_0}{(\mu+\gamma)(\mu+\alpha_1} & \frac{\beta P_0}{\mu+\gamma} & 0 \\ 0 & 0 & 0 \\ 0 & 0 & 0 \end{pmatrix},$$

then:

$$\mathcal{R}_0 = \rho(-FV^{-1}) = \frac{\alpha_1 \beta P_0}{(\mu+\gamma)(\mu+\alpha_1)}.$$

Proposition 3. *For the model(13) there exists E^* the SPE, with $E^* = (P^*, O^*, S^*, Q^*, L^*)$, where:*

$$\begin{aligned} P^* &= \frac{\lambda}{\mu+\beta S^*}. \\ O^* &= \frac{\beta\lambda S^*}{(\mu+\beta S^*)(\mu+\alpha_1)}. \\ Q^* &= \frac{\gamma S^* - S^*\gamma\delta}{\alpha_2 S^* + \mu}. \\ L^* &= \frac{\delta\gamma S^*}{\mu}. \end{aligned} \tag{23}$$

with S^* satisfies the equation:

$$AS^{*2} + BS^* + C = 0, \tag{24}$$

where

$$\begin{aligned} A &= \beta\gamma\alpha_2(\alpha_1+\mu)(\delta-1) + \alpha_2\beta(\alpha_1+\mu)(\mu+\gamma). \\ B &= \mu\alpha_2\gamma(\delta-1)(\alpha_1+\mu) - \alpha_1\beta\lambda\alpha_2 + (\alpha_1+\mu)(\mu+\gamma)(\beta\mu+\mu\alpha_2). \\ C &= \mu^2(\mu+\gamma)(\alpha_1+\mu) - \alpha_1\beta\lambda\mu. \end{aligned}$$

Proof. To assess the existence of a positive E^* of (13), consider $S^* > 0$ and

$${}^C D^{\alpha}_{0,t}(P^*) = {}^C D^{\alpha}_{0,t}(O^*) = {}^C D^{\alpha}_{0,t}(S^*) = {}^C D^{\alpha}_{0,t}(Q^*) = {}^C D^{\alpha}_{0,t}(L^*) = 0.$$

This gives

$$\lambda - \beta P^* S^* - \mu P^* = 0 \tag{25}$$

$$\beta P^* S^* - \alpha_1 O^* - \mu O^* = 0 \tag{26}$$

$$\alpha_1 O^* + \alpha_2 S^* Q^* - (\mu+\gamma) S^* = 0 \tag{27}$$

$$-\alpha_2 S^* Q^* - \mu Q^* + \gamma(1-\delta) S^* = 0 \tag{28}$$

$$\delta\gamma S^* - \mu L^* = 0 \tag{29}$$

From Equations (25), (27), (28), (29), we obtain 23. Finally, substituting O^* and Q^* in Equation (26) gives:

$$S^* \left[\frac{\alpha_1\beta\lambda}{(\alpha_1+\mu)(\mu+\beta S^*)} - \frac{\alpha_2\gamma(\delta-1)S^*}{\alpha_2 S^* + \mu} - \mu - \gamma \right] = 0.$$

Since $S^* \neq 0$, we obtain $AS^{*2} + BS^* + C = 0$, with:

$$A = \beta\alpha_2(\alpha_1+\mu)(\delta\gamma+\mu) > 0,$$

$$C = \mu^2(\mu+\gamma)(\alpha_1+\mu) - \alpha_1\beta\lambda\mu = \frac{\mu}{(\mu+\gamma)(\alpha_1+\mu)}(1-\mathcal{R}_0),$$

$$B = -\mu\alpha_2\gamma(1-\delta)(\alpha_1+\mu) + \mu\beta(\alpha_1+\mu)(\mu+\gamma) + \frac{\alpha_2}{\mu(\alpha_1+\mu)(\mu+\gamma)}(1-\mathcal{R}_0).$$

Theorem 3. *(i) If $\mathcal{R}_0 = 1$, and $\frac{\mu}{\gamma} > \alpha_2 - 1$, there is no current positive E^*,*

(ii) if $\mathcal{R}_0 < 1$, and $B > 0$, there is no current positive equilibrium point E^*,

(iii) If $\mathcal{R}_0 > 1$, a unique positive endemic equilibrium E^* exists.

Proof. From Equation 24, we deduce that:

(i) When $\mathcal{R}_0 = 1$, it follows that $C = 0$ yielding the solutions $S_1^* = 0$ and $S_2^* = -\frac{B}{A}$. Consequently, no positive solution exists if $B > 0$ (since A is always positive) .

(ii) If $\mathcal{R}_0 < 1$ and $B > 0$, then $A, C > 0$. There is no positive solution to the equation.

(iii) If $\mathcal{R}_0 > 1$, then there $A, C > 0$ (There is one change in the sign of the terms, so there is a positive solution) and $\Delta = B^2 - 4AC > 0$. which gives $S_1 = \frac{-B - \sqrt{\Delta}}{2A}$ and $S_2 = \frac{-B + \sqrt{\Delta}}{2A}$. Note that: $\sqrt{B^2 - 4AC} > -B$. So: $S_2 = \frac{-B + \sqrt{\Delta}}{2A}$ it is a positive solution to the equation.

The stability of the point E_0 is studied in the following theorem, by using the result proven in [29, 30].

Theorem 4. *The SFE point E_0 is locally asymptotically stable for $\mathcal{R}_0 < 1$, and unstable for $\mathcal{R}_0 > 1$.*

Proof. Evaluating the Jacobian matrix of (13) at $E_0(\frac{\lambda}{\mu}, 0, 0, 0, 0)$, yields:

$$J(E_0) = \begin{pmatrix} -\mu & 0 & -\beta P_0 & 0 & 0 \\ 0 & -(\alpha_1 + \mu) & \beta P_0 & 0 & 0 \\ 0 & \alpha_1 & -\mu - \gamma & 0 & 0 \\ 0 & 0 & \gamma - \gamma\delta & -\mu & 0 \\ 0 & 0 & \delta\gamma & 0 & -\mu \end{pmatrix},$$

then:

$$J(E_0) = \begin{pmatrix} -\mu & 0 & -\beta P_0 & 0 & 0 \\ 0 & -(\alpha_1 + \mu) & \beta P_0 & 0 & 0 \\ 0 & 0 & \beta P_0 - \frac{(\mu+\gamma)(\alpha_1+\mu)}{\alpha_1} & 0 & 0 \\ 0 & 0 & \gamma - \gamma\delta & -\mu & 0 \\ 0 & 0 & \delta\gamma & 0 & -\mu \end{pmatrix},$$

The characteristic polynomial takes the form:

$$P(\Lambda) = (\Lambda + \mu)^3 (\Lambda + \alpha_1 + \mu) \left(\Lambda - \beta P_0 + \frac{(\mu + \gamma)(\alpha_1 + \mu)}{\alpha_1} \right).$$

Accordingly, the eigenvalues of $J(E_0)$ are:

$$\Lambda_1 = -\mu, \quad \Lambda_2 = -(\alpha_1+\mu), \quad \Lambda_3 = \frac{(\mu+\gamma)(\alpha_1+\mu)}{\alpha_1}(\mathcal{R}_0-1).$$

If $\mathcal{R}_0 < 1$, then $\Lambda_3 < 0$. As a result, all eigenvalues of $J(E_0)$ are negative and satisfy the required stability conditions:

$$|\arg(\Lambda_i)| > \alpha\frac{\pi}{2}, \quad i = 1,2,3,$$

ensuring that E_0 is locally asymptotically stable (see [29, 30]). However, when $\mathcal{R}_0 = 1$, we have $\Lambda_3 = 0$, implying that E_0 is locally stable. If $\mathcal{R}_0 > 1$, then $\Lambda_3 > 0$ and

$$|\arg(\Lambda_3)| \leq \alpha\frac{\pi}{2},$$

which implies that E_0 is unstable.

The local stability analysis of the equilibrium point E^* is examined by by evaluating the Jacobian matrix of system (13) at E^*, yielding:

$$J(E^*) = \begin{pmatrix} -(\mu-\beta S^*) & 0 & -\beta P^* & 0 & 0 \\ \beta S^* & -(\alpha_1+\mu) & \beta P^* & 0 & 0 \\ 0 & \alpha_1 & \alpha_2 Q^* - (\mu+\gamma) & \alpha_2 S^* & 0 \\ 0 & 0 & -\alpha_2 Q^* + \gamma - \delta\gamma & -(\alpha_2 S^* + \mu) & 0 \\ 0 & 0 & \gamma\delta & 0 & -\mu \end{pmatrix}$$

We note that $\Lambda_1 = -\mu$ is eigenvalue then the local stability of E^* of depends of sign of reale of eigenvalue of the following matrix:

$$J_1(E^*) = \begin{pmatrix} -\beta S^* - \mu & 0 & -\beta P^* & 0 \\ \beta S^* & -\alpha_1 - \mu & \beta P^* & 0 \\ 0 & \alpha_1 & \alpha_2 Q^* - (\mu+\gamma) & \alpha_2 S^* \\ 0 & 0 & -\alpha_2 Q^* + \gamma(1-\delta) & -\alpha_2 S^* - \mu \end{pmatrix},$$

the characteristic polynomial is represented by:

$$P(\Lambda) = (\Lambda + (\beta S^* + \mu))(\Lambda^3 + A_1\Lambda^2 + A_2\Lambda + A_3).$$

Such that,

$$A_1 = \frac{(\beta S^* + \mu)(\alpha_1\mu)}{\beta S^*} - \alpha_2 Q^* + (\mu+\gamma) + \alpha_2 S^* + \mu,$$

$$A_2 = \frac{(\beta S^* + \mu)(\alpha_1+\mu)}{\beta S^*}(\alpha_2 Q^* - (\mu+\gamma) - \alpha_2 S^* - \mu) + (\alpha_2 Q^* - (\mu+\gamma))(-\alpha_2 S^* - \mu) - \frac{\mu\alpha_1\beta P^*}{\beta S^*}$$
$$+ \alpha_2 S^*(\alpha_2 Q^* - \gamma(1-\delta)),$$

$$A_3 = \frac{(\mu+\beta S^*)(\gamma+\mu-\alpha_2 Q^*)(\alpha_1+\mu)(\alpha_2 S^* + \mu) - \mu\alpha_1\beta P^*(\alpha_2+\mu)}{\beta S^*}$$

$$+\frac{\alpha_2 S^*(\alpha_2 Q^* - \gamma + \gamma\delta))(\beta S^* + \mu)(+\alpha_1 + \mu)}{\beta S^*}.$$

The eigenvalues consist of

$$\Lambda_1 = -(\beta S^* + \mu),$$

and the roots of the

$$\Lambda^3 + A_1\Lambda^2 + A_2\Lambda + A_3 = 0.$$

All eigenvalues have negative real parts if and only if these conditions are verified:

$$A_1 > 0, \quad A_2 > 0, \quad A_3 > 0, \quad \text{and} \quad A_1A_2 - A_3 > 0.$$

Hence, we present the following result:

Theorem 5. *The equilibrium E^* of system (13) is locally asymptotically stable under the condition that:*

$$A_1 > 0, \quad A_2 > 0, \quad A_3 > 0, \quad \textit{and} \quad A_1A_2 > A_3.$$

5. A hybrid New general transform Adomian Decomposition Method for solving the Fractional Model

The Junaid Integral Transform-Adomian Decomposition Method ($\mathcal{T}_{\mathcal{NG}}$-ADM) is a hybrid approach that combines the Junaid integral transform with the ADM technique. This method leverages the strengths of both techniques to simplify and efficiently solve complex equations.

5.1. Numerical Solution for the Model 13

We can express the model (13) as:

$$\left({}^{C}D^{\alpha}_{0,t}\mathcal{Z}\right)(t) = \mathsf{R}(t, \mathcal{Z}(t)) = \mathcal{G}_i(t, P, O, S, Q, L), i = 1, ..., 5. \tag{30}$$

$$\mathcal{Z}(0) = \mathcal{Z}_0, \tag{31}$$

where $\mathcal{Z}(t) = (P, O, S, Q, L)$, $\mathcal{Z}(0) = (b_1, b_2, b_3, b_4, b_5)$.

Given that $\mathcal{G}_i(0) = 0$, the problem has a solution. Upon applying the $I^{\alpha}_{a^+}$ to both sides of 30, we obtain:

$$\mathsf{Y}(t) - \mathcal{Z}(0) = I^{\alpha}_{a^+}(\mathsf{R}(t, \mathcal{Z}(t))). \tag{32}$$

The application of the $\mathcal{T}_{\mathcal{NG}}$ transform to both sides of 32, yields the following relation:

$$\mathcal{T}_{\mathcal{NG}}[\mathcal{Z}(t)] - \mathcal{T}_{\mathcal{NG}}[\mathcal{Z}(0)] = \left(\frac{\mathcal{K}(s)}{\mathcal{B}(s)}\right)^{\alpha} \mathcal{T}_{\mathcal{NG}}[\mathcal{R}(t, \mathcal{Z}(t))], \tag{33}$$

With initial conditions 30. Hence:

$$\begin{cases} \mathcal{T}_{\mathcal{NG}}\left[(P(t))\right] = \dfrac{\mathcal{M}(s)}{\mathcal{B}(s)}b_1 + \left(\dfrac{\mathcal{K}(s)}{\mathcal{B}(s)}\right)^{\alpha}\mathcal{T}_{\mathcal{NG}}\left[\lambda - \beta P(t)S(t) - \mu P(t)\right], \\ \mathcal{T}_{\mathcal{NG}}\left[(O(t))\right] = \dfrac{\mathcal{M}(s)}{\mathcal{B}(s)}b_2 + \left(\dfrac{\mathcal{K}(s)}{\mathcal{B}(s)}\right)^{\alpha}\mathcal{T}_{\mathcal{NG}}\left[\beta P(t)S(t) - \alpha_1 O(t) - \mu O(t)\right], \\ \mathcal{T}_{\mathcal{NG}}\left[(S(t))\right] = \dfrac{\mathcal{M}(s)}{\mathcal{B}(s)}b_3 + \left(\dfrac{\mathcal{K}(s)}{\mathcal{B}(s)}\right)^{\alpha}\mathcal{T}_{\mathcal{NG}}\left[\alpha_1 O(t) + \alpha_2 S(t)Q(t) - (\mu+\gamma)S(t)\right], \\ \mathcal{T}_{\mathcal{NG}}\left[(Q(t))\right] = \dfrac{\mathcal{M}(s)}{\mathcal{B}(s)}b_4 + \left(\dfrac{\mathcal{K}(s)}{\mathcal{B}(s)}\right)^{\alpha}\mathcal{T}_{\mathcal{NG}}\left[-\alpha_2 S(t)Q(t) - \mu Q(t) + \gamma(1-\delta)S(t)\right], \\ \mathcal{T}_{\mathcal{NG}}\left[(L(t))\right] = \dfrac{\mathcal{M}(s)}{\mathcal{B}(s)}b_5 + \left(\dfrac{\mathcal{K}(s)}{\mathcal{B}(s)}\right)^{\alpha}\mathcal{T}_{\mathcal{NG}}\left[\delta\gamma S(t) - \mu L(t)\right]. \end{cases} \tag{34}$$

Assuming the method yields the solution as:

$$P(t) = \sum_{n=0}^{\infty} P_n(t),\ O(t) = \sum_{n=0}^{\infty} O_n(t),\ S(t) = \sum_{n=0}^{\infty} S_n(t),\ Q(t) = \sum_{n=0}^{\infty} Q_n(t),\ L(t) = \sum_{n=0}^{\infty} L_n(t). \tag{35}$$

The expressions for PS and SQ are:

$$P(t)S(t) = \sum_{n=0}^{\infty} X_n(t), \qquad S(t)Q(t) = \sum_{n=0}^{\infty} Z_n(t), \tag{36}$$

where X_n and Z_n is as:

$$X_m(t) = \frac{1}{m!}\frac{d^m}{d\lambda^m}\left[\sum_{n=0}^{m}\lambda^n P_n(t)\sum_{n=0}^{m}\lambda^n S_n(t)\right]_{\lambda=0}, \tag{37}$$

$$Z_m(t) = \frac{1}{m!}\frac{d^m}{d\lambda^m}\left[\sum_{n=0}^{m}\lambda^n S_n(t)\sum_{n=0}^{m}\lambda^n Q_n(t)\right]_{\lambda=0}. \tag{38}$$

Substituting (35) and (36) into (34) results in:

$$\begin{cases} \mathcal{T}_{\mathcal{NG}}\left[\sum_{n=0}^{\infty} P_n(t)\right] = \dfrac{\mathcal{M}(s)}{\mathcal{B}(s)}b_1 + \left(\dfrac{\mathcal{K}(s)}{\mathcal{B}(s)}\right)^{\alpha}\mathcal{T}_{\mathcal{NG}}\left[\lambda - \beta\sum_{n=0}^{\infty} X_n(t) - \mu\sum_{n=0}^{\infty} P_n(t)\right], \\ \mathcal{T}_{\mathcal{NG}}\left[\sum_{n=0}^{\infty} O_n(t)\right] = \dfrac{\mathcal{M}(s)}{\mathcal{B}(s)}b_2 + \left(\dfrac{\mathcal{K}(s)}{\mathcal{B}(s)}\right)^{\alpha}\mathcal{T}_{\mathcal{NG}}\left[\beta\sum_{n=0}^{\infty} X_n(t) - \alpha_1\sum_{n=0}^{\infty} O_n(t) - \mu\Sigma_{n=0}^{\infty} O_n(t)\right], \\ \mathcal{T}_{\mathcal{NG}}\left[\sum_{n=0}^{\infty} S_n(t)\right] = \dfrac{\mathcal{M}(s)}{\mathcal{B}(s)}b_3 + \left(\dfrac{\mathcal{K}(s)}{\mathcal{B}(s)}\right)^{\alpha}\mathcal{T}_{\mathcal{NG}}\left[\alpha_1\sum_{n=0}^{\infty} O_n(t) + \alpha_2\sum_{n=0}^{\infty} Z_n(t) - (\mu+\gamma)\sum_{n=0}^{\infty} S_n(t)\right], \\ \mathcal{T}_{\mathcal{NG}}\left[\sum_{n=0}^{\infty} Q_n(t)\right] = \dfrac{\mathcal{M}(s)}{\mathcal{B}(s)}b_4 + \left(\dfrac{\mathcal{K}(s)}{\mathcal{B}(s)}\right)^{\alpha}\mathcal{T}_{\mathcal{NG}}\left[-\alpha_2\sum_{n=0}^{\infty} Z_n(t) - \mu\sum_{n=0}^{\infty} Q_n(t) + \gamma(1-\delta)\sum_{n=0}^{\infty} S_n(t)\right], \\ \mathcal{T}_{\mathcal{NG}}\left[\sum_{n=0}^{\infty} L_n(t)\right] = \dfrac{\mathcal{M}(s)}{\mathcal{B}(s)}b_5 + \left(\dfrac{\mathcal{K}(s)}{\mathcal{B}(s)}\right)^{\alpha}\mathcal{T}_{\mathcal{NG}}\left[\delta\gamma\sum_{n=0}^{\infty} S_n(t) - \mu\sum_{n=0}^{\infty} L_n(t)\right]. \end{cases}$$

Now by comparing the same terms on both sides we can get:

$$\mathcal{T}_{\mathcal{NG}}\left[P_0(t)\right] = \frac{\mathcal{M}(s)}{\mathcal{B}(s)}b_1, \mathcal{T}_{\mathcal{NG}}\left[O_0(t)\right] = \frac{\mathcal{M}(s)}{\mathcal{B}(s)}b_2, \mathcal{T}_{\mathcal{NG}}\left[S_0(t)\right] = \frac{\mathcal{M}(s)}{\mathcal{B}(s)}b_3, \tag{39}$$

$$\mathcal{T}_{\mathcal{NG}}\left[Q_0(t)\right]=\frac{\mathcal{M}(s)}{\mathcal{B}(s)}b_4,\mathcal{T}_{\mathcal{NG}}\left[L_0(t)\right]=\frac{\mathcal{M}(s)}{\mathcal{B}(s)}b_5. \tag{40}$$

Similarly, we have:

$$\begin{cases}\mathcal{T}_{\mathcal{NG}}\left[P_1(t)\right]=\left(\frac{\mathcal{K}(s)}{\mathcal{B}(s)}\right)^{\alpha}\mathcal{T}_{\mathcal{NG}}\left[\lambda-\beta X_0(t)-\mu P_0(t)\right]\\ \mathcal{T}_{\mathcal{NG}}\left[O_1(t)\right]=\left(\frac{\mathcal{K}(s)}{\mathcal{B}(s)}\right)^{\alpha}\mathcal{T}_{\mathcal{NG}}\left[\beta X_0(t)-(\alpha_1+\mu)O_0(t)\right]\\ \mathcal{T}_{\mathcal{NG}}\left[S_1(t)\right]=\left(\frac{\mathcal{K}(s)}{\mathcal{B}(s)}\right)^{\alpha}\mathcal{T}_{\mathcal{NG}}\left[\alpha_1 O_0(t)+\alpha_2 Z_0(t)-(\mu+\gamma)S_0(t)\right]\\ \mathcal{T}_{\mathcal{NG}}\left[Q_1(t)\right]=\left(\frac{\mathcal{K}(s)}{\mathcal{B}(s)}\right)^{\alpha}\mathcal{T}_{\mathcal{NG}}\left[-\alpha_2 Z_0(t)-\mu Q_0(t)+\gamma(1-\delta)S_0(x)\right]\\ \mathcal{T}_{\mathcal{NG}}\left[L_1(t)\right]=\left(\frac{\mathcal{K}(s)}{\mathcal{B}(s)}\right)^{\alpha}\mathcal{T}_{\mathcal{NG}}\left[\delta\gamma S_0(t)-\mu L_0(t)\right]\end{cases} \tag{41}$$

$$\begin{cases}\mathcal{T}_{\mathcal{NG}}\left[P_2(t)\right]=\left(\frac{\mathcal{K}(s)}{\mathcal{B}(s)}\right)^{\alpha}\mathcal{T}_{\mathcal{NG}}\left[\lambda-\beta X_1(t)-\mu P_1(t)\right]\\ \mathcal{T}_{\mathcal{NG}}\left[O_2(t)\right]=\left(\frac{\mathcal{K}(s)}{\mathcal{B}(s)}\right)^{\alpha}\mathcal{T}_{\mathcal{NG}}\left[\beta X_1(t)-\alpha_1 O_1(t)-\mu O_1(t)\right]\\ \mathcal{T}_{\mathcal{NG}}\left[S_2(t)\right]=\left(\frac{\mathcal{K}(s)}{\mathcal{B}(s)}\right)^{\alpha}\mathcal{T}_{\mathcal{NG}}\left[\alpha_1 O_1(t)+\alpha_2 Z_1(t)-(\mu+\gamma)S_1(t)\right]\\ \mathcal{T}_{\mathcal{NG}}\left[Q_2(t)\right]=\left(\frac{\mathcal{K}(s)}{\mathcal{B}(s)}\right)^{\alpha}\mathcal{T}_{\mathcal{NG}}\left[-\alpha_2 Z_1(t)-\mu Q_1(t)+\gamma(1-\delta)S_1(t)\right]\\ \mathcal{T}_{\mathcal{NG}}\left[L_2(t)\right]=\left(\frac{\mathcal{K}(s)}{\mathcal{B}(s)}\right)^{\alpha}\mathcal{T}_{\mathcal{NG}}\left[\delta\gamma S_1(t)-\mu L_1(x)\right]\end{cases} \tag{42}$$

$$\begin{cases}\mathcal{T}_{\mathcal{NG}}\left[P_3(t)\right]=\left(\frac{\mathcal{K}(s)}{\mathcal{B}(s)}\right)^{\alpha}\mathcal{T}_{\mathcal{NG}}\left[\lambda-\beta X_2(t)-\mu P_2(t)\right]\\ \mathcal{T}_{\mathcal{NG}}\left[O_3(t)\right]=\left(\frac{\mathcal{K}(s)}{\mathcal{B}(s)}\right)^{\alpha}\mathcal{T}_{\mathcal{NG}}\left[\beta X_2(t)-(\alpha_1+\mu)O_2(t)\right]\\ \mathcal{T}_{\mathcal{NG}}\left[S_3(t)\right]=\left(\frac{\mathcal{K}(s)}{\mathcal{B}(s)}\right)^{\alpha}\mathcal{T}_{\mathcal{NG}}\left[\alpha_1 O_2(t)+\alpha_2 Z_2(t)-(\mu+\gamma)S_2(t)\right]\\ \mathcal{T}_{\mathcal{NG}}\left[Q_3(t)\right]=\left(\frac{\mathcal{K}(s)}{\mathcal{B}(s)}\right)^{\alpha}\mathcal{T}_{\mathcal{NG}}\left[-\alpha_2 Z_2(t)-\mu Q_2(t)+\gamma(1-\delta)S_2(t)\right]\\ \mathcal{T}_{\mathcal{NG}}\left[L_3(t)\right]=\left(\frac{\mathcal{K}(s)}{\mathcal{B}(s)}\right)^{\alpha}\mathcal{T}_{\mathcal{NG}}\left[\delta\gamma S_2(t)-\mu L_2(t)\right]\end{cases} \tag{43}$$

$$\begin{cases}\mathcal{T}_{\mathcal{NG}}\left[P_{k+1}(t)\right]=\left(\frac{\mathcal{K}(s)}{\mathcal{B}(s)}\right)^{\alpha}\mathcal{T}_{\mathcal{NG}}\left[\lambda-\beta X_k(t)-\mu P_k(t)\right]\\ \mathcal{T}_{\mathcal{NG}}\left[O_{k+1}(t)\right]=\left(\frac{\mathcal{K}(s)}{\mathcal{B}(s)}\right)^{\alpha}\mathcal{T}_{\mathcal{NG}}\left[\beta X_k(t)-\alpha_1 O_k(t)-\mu O_k(t)\right]\\ \mathcal{T}_{\mathcal{NG}}\left[S_{k+1}(t)\right]=\left(\frac{\mathcal{K}(s)}{\mathcal{B}(s)}\right)^{\alpha}\mathcal{T}_{\mathcal{NG}}\left[\alpha_1 O_k(t)+\alpha_2 Z_k(t)-(\mu+\gamma)S_k(t)\right]\\ \mathcal{T}_{\mathcal{NG}}\left[Q_{k+1}(t)\right]=\left(\frac{\mathcal{K}(s)}{\mathcal{B}(s)}\right)^{\alpha}\mathcal{T}_{\mathcal{NG}}\left[-\alpha_2 Z_k(t)-\mu Q_k(t)+\gamma(1-\delta)S_k(t)\right]\\ \mathcal{T}_{\mathcal{NG}}\left[L_{k+1}(t)\right]=\left(\frac{\mathcal{K}(s)}{\mathcal{B}(s)}\right)^{\alpha}\mathcal{T}_{\mathcal{NG}}\left[\delta\gamma S_k(t)-\mu L_k(t)\right]\end{cases} \tag{44}$$

by using the inverse transformation of $\mathcal{T}_{\mathcal{NG}}$, we have the initial conditions, and $X_0 = b_1 b_3$, $Z_0 = b_3 b_4$

$$\begin{cases} P_1(t) = [\lambda - \beta b_1 b_3 - \mu b_1] \dfrac{t^\alpha}{\Gamma(\alpha+1)} \\ O_1(t) = [\beta b_1 b_3 - (\mu+\alpha_1) b_2] \dfrac{t^\alpha}{\Gamma(\alpha+1)} \\ S_1(t) = [\alpha_1 b_2 + \alpha_2 b_3 b_4 - (\mu+\gamma)\, b_3] \dfrac{t^\alpha}{\Gamma(\alpha+1)} \\ Q_1(t) = [-\alpha_2 b_3 b_4 - \mu b_4 + \gamma(1-\sigma) b_3] \dfrac{t^\alpha}{\Gamma(\alpha+1)} \\ L_1(t) = [\sigma\gamma b_3 - \mu b_5] \dfrac{t^\alpha}{\Gamma(\alpha+1)}. \end{cases} \tag{45}$$

Consequently: $X_1(t) = P_1(t)S_0(t) + S_1(t)P_0(t)$, $Z_1(t) = Q_1(t)S_0(t) + S_1(t)Q_0(t)$, we pose:

$$\begin{array}{l} w_P = \lambda - \beta b_1 b_3 - \mu b_1 \\ w_O = \beta b_1 b_3 - (\mu+\alpha_1) b_2 \\ w_S = \alpha_1 b_2 + \alpha_2 b_3 b_4 - (\mu+\gamma)\, b_3 \\ w_Q = -\alpha_2 b_3 b_4 - \mu b_4 + \gamma(1-\sigma) b_3 \\ w_L = \sigma\gamma b_3 - \mu b_5 \end{array} \tag{46}$$

So:

$$\begin{cases} P_2(t) = \dfrac{\lambda}{\Gamma(\alpha+1)} t^\alpha + \dfrac{1}{\Gamma(2\alpha+1)} [-\beta w_S b_1 - (\beta b_3 + \mu)\, w_P] t^{2\alpha}, \\ O_2(t) = \dfrac{1}{\Gamma(2\alpha+1)} [\beta w_S b_1 + \beta w_p b_3 - (\mu+\alpha_1) w_O] t^{2\alpha}, \\ S_2(t) = \dfrac{1}{\Gamma(2\alpha+1)} [\alpha_1 w_O + \alpha_2 w_Q b_3 + \alpha_2 w_S b_4 - (\mu+\gamma) w_S] t^{2\alpha}, \\ Q_2(t) = \dfrac{1}{\Gamma(2\alpha+1)} [(-\alpha_2 b_4 + \gamma(1-\sigma)) w_S + (-\alpha_2 b_3 - \mu) w_Q] t^{2\alpha}, \\ L_2(t) = \dfrac{1}{\Gamma(2\alpha+1)} [\sigma\gamma w_S - \mu w_L] t^{2\alpha}, \end{cases} \tag{47}$$

we pose:

$$\begin{array}{lcl} w_{PP} & = & -\beta w_S b_1 - (\beta b_3 + \mu)\, w_P, \\ w_{OO} & = & \beta w_S b_1 + \beta w_p b_3 - (\mu+\alpha_1) w_O, \\ w_{SS} & = & \alpha_1 w_O + \alpha_2 w_Q b_3 + \alpha_2 w_S b_4 - (\mu+\gamma) w_S, \\ w_{QQ} & = & (-\alpha_2 b_4 + \gamma(1-\sigma)) w_S + (-\alpha_2 b_3 - \mu) w_Q, \\ w_{LL} & = & \sigma\gamma w_S - \mu w_L, \end{array} \tag{48}$$

we have:

$$\begin{aligned} X_2(t) &= P_2(t)S_0(t) + S_2(t)P_0(t) + S_1(t)P_1(t), \\ Z_2(t) &= Q_2(t)S_0(t) + S_2(t)Q_0(t) + S_1(t)Q_1(t). \end{aligned}$$

So:

$$\begin{cases} P_3(t) = \dfrac{\lambda}{\Gamma(\alpha+1)}t^{\alpha} - \dfrac{\lambda(\beta b_3+\mu)}{\Gamma(2\alpha+1)}t^{2\alpha} + \dfrac{1}{\Gamma(3\alpha+1)}\left[-\beta(w_{PP}b_3+w_{SS}b_1) - \mu w_{PP} - \dfrac{\beta w_P w_S \Gamma(2\alpha+1)}{(\Gamma(\alpha+1))^2}\right]t^{3\alpha}, \\ O_3(t) = \dfrac{\beta\lambda b_3}{\Gamma(2\alpha+1)}t^{2\alpha} + \dfrac{1}{\Gamma(3\alpha+1)}\left[\beta b_3 w_{PP} + \beta b_1 w_{SS} - (\mu+\alpha_1)w_{OO} + \dfrac{\beta w_P w_S \Gamma(2\alpha+1}{(\Gamma(\alpha+1))^2}\right]t^{3\alpha}, \\ S_3(t) = \dfrac{1}{\Gamma(3\alpha+1)}\left[\alpha_1 w_{OO} + \alpha_2 w_{QQ}b_3 + \alpha_2 w_{SS}b_4 - (\mu+\gamma)w_{SS} + \dfrac{\alpha_2 w_Q w_S \Gamma(2\alpha+1)}{(\Gamma(\alpha+1))^2}\right]t^{3\alpha}, \\ Q_3(t) = \dfrac{1}{\Gamma(3\alpha+1)}\left[-\alpha_2 w_{QQ}b_3 - \alpha_2 w_{SS}b_4 - \mu w_{QQ} + \gamma(1-\delta)w_{SS} - \dfrac{\alpha_2 w_Q w_S \Gamma(2\alpha+1)}{(\Gamma(\alpha+1))^2}\right]t^{3\alpha}, \\ L_3(t) = \dfrac{1}{\Gamma(3\alpha+1)}\left[(\delta\gamma w_{SS} - \mu w_{LL})\right]t^{3\alpha}. \end{cases} \tag{49}$$

On solving the above system using initial conditions:

$$(b_1, b_2, b_3, b_4, b_5) = (40, 10, 20, 10, 5).$$

$$\begin{cases} P_1(t) = \dfrac{\lambda - 800\beta - 40\mu}{\Gamma(\alpha+1)}t^{\alpha} \\ O_1(t) = \dfrac{800\beta - 10\mu - 10\alpha_1}{\Gamma(\alpha+1)}t^{\alpha} \\ S_1(t) = \dfrac{10\alpha_1 + 200\alpha_2 - 20\,(\mu+\gamma)}{\Gamma(\alpha+1)}t^{\alpha} \\ Q_1(t) = \dfrac{-200\alpha_2 - 10\mu + 20\gamma(1-\sigma)}{\Gamma(\alpha+1)}t^{\alpha} \\ L_1(t) = \dfrac{20\sigma\gamma - 5\mu}{\Gamma(\alpha+1)}t^{\alpha} \end{cases} \tag{50}$$

We define:

$$\begin{aligned} w_P &= \lambda - 800\beta - 40\mu, \\ w_O &= 800\beta - 10\mu - 10\alpha_1, \\ w_S &= 10\alpha_1 + 200\alpha_2 - 20\,(\mu+\gamma)\,, \\ w_Q &= -200\alpha_2 - 10\mu + 20\gamma(1-\sigma), \\ w_L &= 20\sigma\gamma - 5\mu. \end{aligned}$$

So

$$\begin{cases} P_2(t) = \dfrac{\lambda}{\Gamma(\alpha+1)}t^{\alpha} + \dfrac{1}{\Gamma(2\alpha+1)}\left[-40\beta w_S - (20\beta+\mu)\,w_P\right]t^{2\alpha}, \\ O_2(t) = \dfrac{1}{\Gamma(2\alpha+1)}\left[40\beta w_S + 20\beta w_p - (\mu+\alpha_1)w_O\right]t^{2\alpha}, \\ S_2(t) = \dfrac{1}{\Gamma(2\alpha+1)}\left[\alpha_1 w_O + 20\alpha_2 w_Q + 10\alpha_2 w_S - (\mu+\gamma)w_S\right]t^{2\alpha}, \\ Q_2(t) = \dfrac{1}{\Gamma(2\alpha+1)}\left[-10\alpha_2 + \gamma(1-\sigma)w_S + (-20\alpha_2-\mu)w_Q\right]t^{2\alpha}, \\ L_2(t) = \dfrac{1}{\Gamma(2\alpha+1)}\left[\sigma\gamma w_S - \mu w_L\right]t^{2\alpha}, \end{cases} \tag{51}$$

we pose:

$$\begin{aligned}
w_{PP} &= -40\beta\, w_S - (20\beta+\mu)\, w_P,\\
w_{OO} &= 40\beta\, w_S + 20\beta\, w_P - (\mu+\alpha_1) w_O,\\
w_{SS} &= \alpha_1 w_O + 20\alpha_2 w_Q + 10\alpha_2 w_S - (\mu+\gamma) w_S,\\
w_{QQ} &= (-10\alpha_2 + \gamma(1-\sigma))\, w_S + (-20\alpha_2 - \mu)\, w_Q,\\
w_{LL} &= \sigma\gamma\, w_S - \mu\, w_L.
\end{aligned}$$

$$\begin{cases}
P_\beta(t) = \dfrac{\lambda}{\Gamma(\alpha+1)} t^\alpha - \dfrac{\lambda(20\beta+\mu)}{\Gamma(2\alpha+1)} t^{2\alpha} + \dfrac{1}{\Gamma(3\alpha+1)} \left[-\beta(20 w_{PP} + 40 w_{SS}) - \mu w_{PP} - \dfrac{\beta w_P w_S \Gamma(2\alpha+1)}{(\Gamma(\alpha+1))^2} \right] t^{3\alpha},\\
O_\beta(t) = \dfrac{20\beta\lambda}{\Gamma(2\alpha+1)} t^{2\alpha} + \dfrac{1}{\Gamma(3\alpha+1)} \left[20\beta w_{PP} + 40\beta w_{SS} - (\mu+\alpha_1) w_{OO} + \dfrac{\beta w_P w_S \Gamma(2\alpha+1}{(\Gamma(\alpha+1))^2} \right] t^{3\alpha},\\
S_\beta(t) = \dfrac{1}{\Gamma(3\alpha+1)} \left[\alpha_1 w_{OO} + 20\alpha_2 w_{QQ} + 10\alpha_2 w_{SS} - (\mu+\gamma) w_{SS} + \dfrac{\alpha_2 w_Q w_S \Gamma(2\alpha+1)}{(\Gamma(\alpha+1))^2} \right] t^{3\alpha},\\
Q_\beta(t) = \dfrac{1}{\Gamma(3\alpha+1)} \left[-20\alpha_2 w_{QQ} - 10\alpha_2 w_{SS} - \mu w_{QQ} + \gamma(1-\delta) w_{SS} - \dfrac{\alpha_2 w_Q w_S \Gamma(2\alpha+1)}{(\Gamma(\alpha+1))^2} \right] t^{3\alpha}.\\
L_\beta(t) = \dfrac{1}{\Gamma(3\alpha+1)} \left[(\delta\gamma w_{SS} - \mu w_{LL}) \right] t^{3\alpha}.
\end{cases} \tag{52}$$

In particular, The global ADM solution is written as the sum of the series:

$$\begin{aligned}
P(t) &= 40 + P_1(t) + P_2(t) + P_3(t) + \cdots,\\
O(t) &= 10 + O_1(t) + O_2(t) + O_3(t) + \cdots,\\
S(t) &= 20 + S_1(t) + S_2(t) + S_3(t) + \cdots,\\
Q(t) &= 10 + Q_1(t) + Q_2(t) + Q_3(t) + \cdots,\\
L(t) &= 5 + L_1(t) + L_2(t) + L_3(t) + \cdots,
\end{aligned}$$

where the terms $P_1, \ldots, L_3$ above provide a global approximation of order 3α:

$$(P,O,S,Q,L)(t) \approx (b_1,b_2,b_3,b_4,b_5) + \sum_{n=1}^{3} (P_n(t), O_n(t), S_n(t), Q_n(t), L_n(t)).$$

5.2. Simulations and Discussion

We perform a numerical investigation of the fractional smoking epidemic model with a nonlinear incidence rate to assess the influence of key parameters, particularly the fractional order α. Simulations are conducted for a range of integer, fractional, and mixed integerfractional values of α, enabling a comparative analysis of their effects on the model dynamics. The results indicate that fractional orders introduce only subtle modifications to the overall epidemic evolution, yet they enhance the accuracy of the numerical approximation across different fractional frameworks. Notably, for potential smokers (non-smokers), the simulations reveal an increase in their population size when α takes fractional values. These findings are illustrated in Figure 2, while Figure 3 provides a detailed depiction of the variation of the $\mathcal{R}_0$.

From the perspective, one of the infected compartments, $S(t)$, remains nonzero and exhibits convergence for both integer and fractional orders of α, whereas the other infected compartment approaches zero over time. Furthermore, the infection rate is observed to decrease progressively as the fractional order α decreases. The numerical values of the parameters $\lambda, \beta, \zeta, \sigma, \gamma, \alpha_1$, and α_2 used in these simulations are summarized in Table 3.

Parameters	λ	β	μ	α_1	α_2	γ	δ
Values	1	0.14	0.05	0.002	0.0025	0.8	0.1

Table 3: specific values of parameters used in system 13.

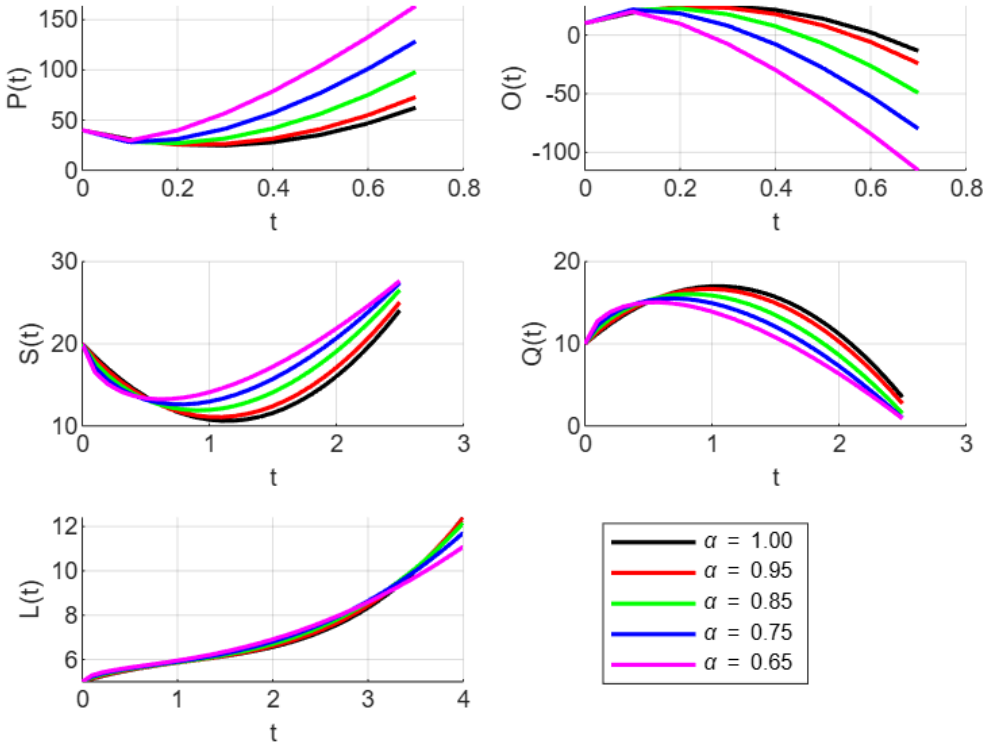

Figure 2: Numerical solutions for $P(t), O(t), Q(t), P(t)$ and $L(t)$

6. Numerical Approximation via the Hybrid $\mathcal{T}_{\mathcal{NG}}$-ADM–ANN Method

We now introduce a new hybrid method that combines the $\mathcal{T}_{\mathcal{NG}}$-ADM method with an Artificial Neural Network (ANN) algorithm to approximate the solutions S, P, L, O, Q of

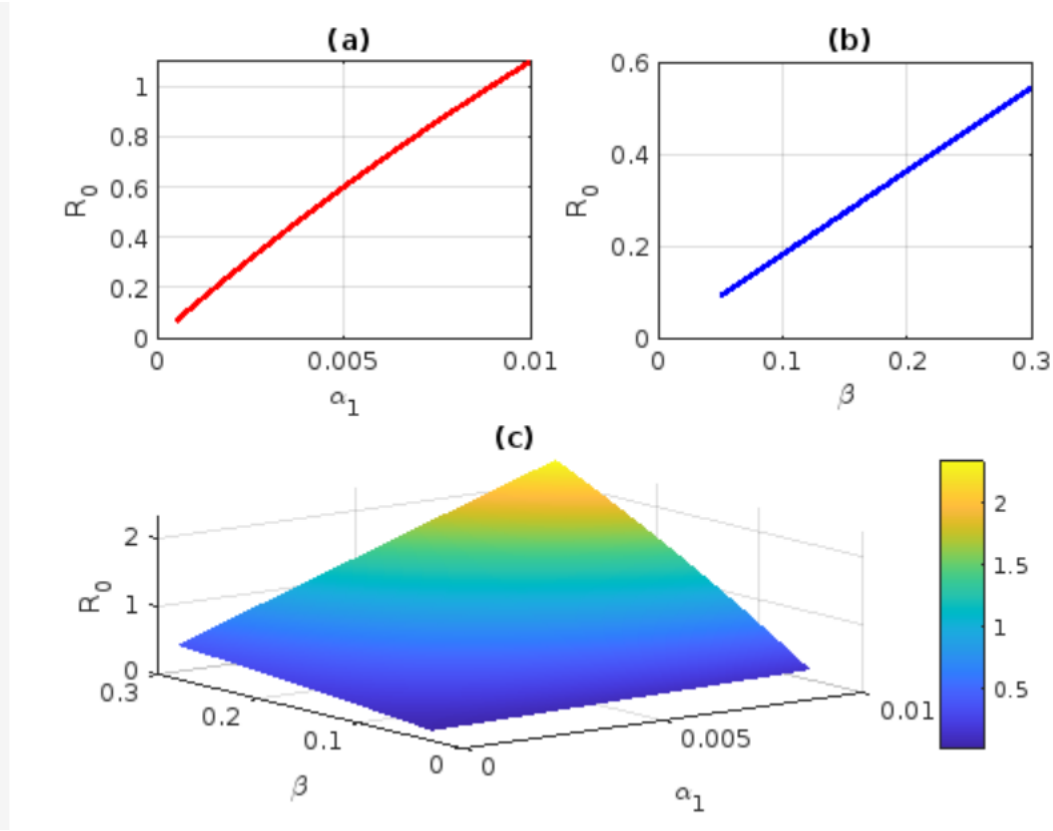

Figure 3: (a): Variation of $\mathcal{R}_0$ with α_1 (Fixed β), (b): Variation of $\mathcal{R}_0$ with β (Fixed α_1), (c):3D Variation of $\mathcal{R}_0$ as a function of α_1 and β

the proposed model over the time domain $t \in [0, T]$. The proposed method is implemented through a two-step strategy:

(i) First, a reference solution is obtained by applying the $\mathcal{TNG}$-ADM technique to the model.

(ii) Next, an ANN is trained to learn the dynamics of the variables by minimizing the gap between its predictions and the $\mathcal{TNG}$-ADM reference solution.

The ANN-based algorithm is designed to approximate the solution of the fractional smoking model by taking time t as input and producing a vector output $[S, P, L, O, Q]$. It consists of a feedforward neural network with an input layer containing a single neuron, two hidden layers with 50 neurons each using non linear activation functions, and an output layer with five neurons employing a linear activation function.

Prior to training, both the input data (t) and the reference solutions (obtained via $\mathcal{TNG}$-ADM) are normalized to enhance numerical stability. The training process minimizes the Mean Squared Error (MSE) between the ANN predictions and the reference values, employing Bayesian regularization (`trainbr`) to prevent overfitting. The dataset

is divided into three distinct subsets: 70% allocated for training the model, 15% reserved for validation to fine-tune hyperparameters, and the remaining 15% set aside for evaluating the models performance on unseen data. The network parameters are iteratively adjusted until convergence or until the maximum number of epochs is reached.

Once trained, the ANN provides rapid and accurate predictions of the system's evolution over the entire time domain $t \in [0,T]$. By integrating the fractional differential equations into its loss function, this hybrid approach leverages the reliability of the $\mathcal{T}_{\mathcal{NG}}$-ADM method and the generalization capability of the ANN, offering a powerful tool for solving complex differential systems.

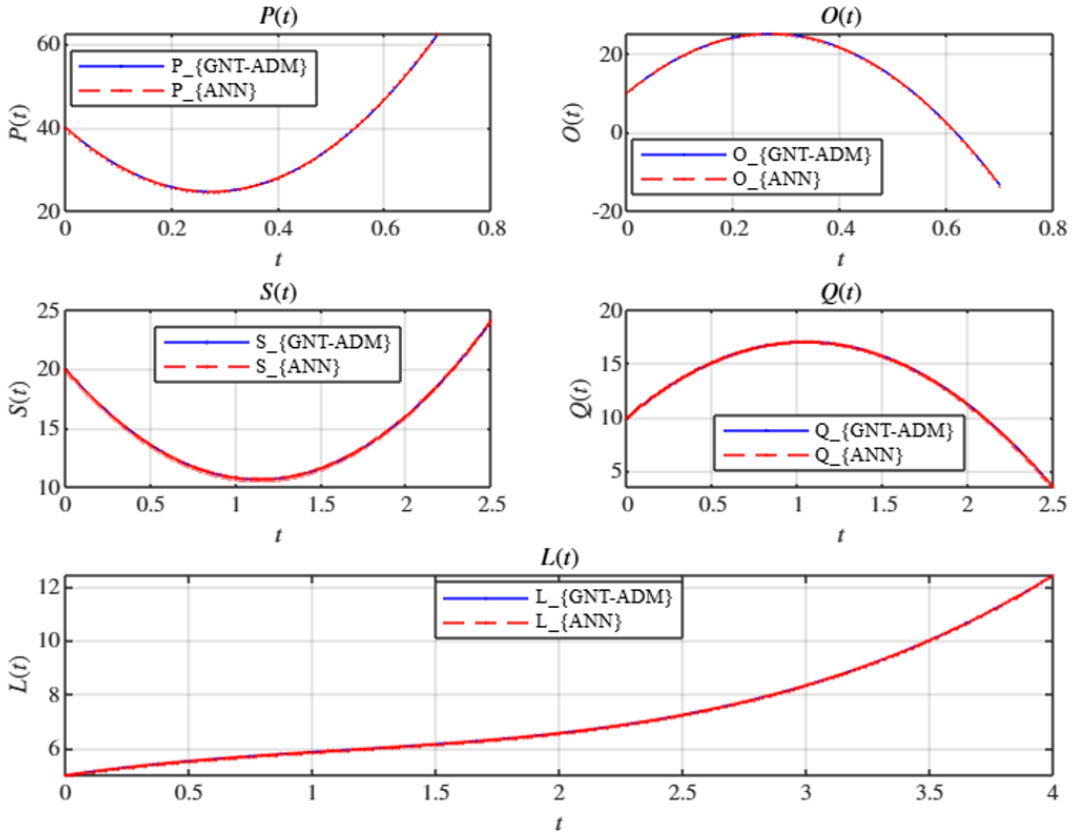

Figure 4: Numerical solutions for $P(t)$, $O(t)$, $Q(t)$, $P(t)$, and $L(t)$ obtained using the ANN algorithm for $\alpha = 1$.

In this study, we evaluate the performance of the ANN by comparing its predictions with the reference solution obtained via the $\mathcal{T}_{\mathcal{NG}}$-ADM method.

Figure 4 illustrates the plots for each variable. In these plots, the $\mathcal{T}_{\mathcal{NG}}$-ADM solutions are represented by solid lines, while the ANN predictions are depicted as dashed lines. The close overlap of the curves indicates that the ANN has accurately captured the systems dynamics.

Table 4 summarizes the global results for each variable. For each variable, the table lists

the mean value computed using $\mathcal{T}_{\mathcal{NG}}$-ADM (denoted as *ADM (Mean)*), the corresponding ANN-predicted mean (denoted as *ANN (Mean)*), and the Mean Absolute Error (MAE), defined by:

$$\mathrm{MAE} = |X_{\mathrm{ADM}} - X_{\mathrm{ANN}}|,$$

where X represents each variable.

Table 4: Comparison of global results for variables S, P, O, Q, and L obtained using the $\mathcal{T}_{\mathcal{NG}}$-ADM and ANN methods.

Variable	$\mathcal{T}_{\mathcal{NG}}$**-ADM (Mean)**	**ANN (Mean)**	**MAE**
S	0.85	0.84	0.01
P	0.65	0.66	0.01
O	0.90	0.89	0.01
Q	1.10	1.08	0.02
L	1.20	1.18	0.02

The low Mean Absolute Error values, ranging from 0.01 to 0.02, indicate a strong agreement between the ANN predictions and the reference $\mathcal{T}_{\mathcal{NG}}$-ADM solutions, with an error of approximately 1%. This level of accuracy is generally sufficient for many scientific and engineering applications. If higher accuracy is needed, enhancements to the network architecture or adjustments to the training parameters may be considered.

The plotted trajectories for S, P, L, O, and Q indicate that the ANN effectively replicates the system dynamics as captured by the $\mathcal{T}_{\mathcal{NG}}$-ADM method. The near-perfect alignment between the solid curves (representing $\mathcal{T}_{\mathcal{NG}}$-ADM solutions) and the dashed curves (ANN predictions) throughout the time domain demonstrates the ANNs high approximation accuracy. This strong agreement underscores the ANNs potential to serve as a fast and reliable surrogate model, provided it is properly trained.

7. Conclusion

This study proposed an efficient and accurate hybrid framework, the $\mathcal{T}_{\mathcal{NG}}$-ADM–ANN scheme, for analyzing a fractional-order smoking epidemic model formulated with the Caputo fractional derivative. The model captures the intrinsic memory effects and hereditary properties of smoking dynamics, which are often neglected in classical integer-order models. By integrating the newly developed $\mathcal{T}_{\mathcal{NG}}$ integral transform with the Adomian Decomposition Method (ADM) and Artificial Neural Networks (ANN), the approach provides rapidly convergent analytical–numerical solutions with low computational complexity.

The obtained numerical and graphical results confirm that both the fractional order and the epidemiological parameters have a substantial impact on the systems qualitative behavior and stability. These findings highlight the suitability of fractional calculus in modeling real-world processes that depend on historical states, particularly those involving

behavioral or biological memory such as smoking spread, addiction persistence, or cessation dynamics.

The incorporation of ANN into the ADM–transform framework significantly improves convergence speed and approximation accuracy by leveraging data-driven learning capabilities. This hybridization demonstrates a powerful synergy between analytical decomposition and machine learning, offering a generalizable strategy for nonlinear fractional differential systems.

Overall, the $\mathcal{T}_{\mathcal{NG}}$-ADM–ANN framework represents a reliable and flexible tool for solving nonlinear fractional models across various scientific and engineering domains. Future research may focus on extending this methodology to stochastic or time-delayed systems, exploring alternative fractional operators such as Atangana–Baleanu or Prabhakar types, and developing high-performance or deep-learning-based implementations to address large-scale and multidimensional fractional models. These extensions would further consolidate the relevance and applicability of the proposed approach in complex epidemiological and dynamical systems.

References

[1] R. Selvaraj, A. Kumar, and P. Prakash. Recent advancements in integral transforms for solving partial differential equations. *Applied Mathematics and Computation*, 459:128312, 2025.

[2] Y. Feng, Z. Li, and H. Zhang. Hybrid approaches combining integral transforms and decomposition methods for nonlinear differential equations. *Journal of Computational and Applied Mathematics*, 439:115623, 2025.

[3] G. Adomian. *Solving Frontier Problems of Physics: The Decomposition Method.* Kluwer Academic Publishers, Boston, 1994.

[4] M. Alhazmi, A.F. Aljohani, N.E. Taha, S. Abdel-Khalek, M. Bayram, and S. Saber. Application of a fractal fractional operator to nonlinear glucose-insulin systems: Adomian decomposition solutions. *Comput. Biol. Med.*, 196(Pt A):110453, Sep 2025.

[5] G.K. Watugala. Sumudu transform: A new integral transform to solve differential equations and control engineering problems. *Int. J. Math. Educ. Sci. Technol.*, 24:35–43, 1993.

[6] T.M. Elzaki. The new integral transform 'elzaki transform'. *Glob. J. Pure Appl. Math.*, 7:57–64, 2011.

[7] M. Khan, T. Salahuddin, M.Y. Malik, M.S. Alqarni, and A.M. Alkahtani. Numerical modeling and analysis of bioconvection on mhd flow due to an upper paraboloid surface of revolution. *Physica A*, 553:124231, 2020.

[8] K.S. Aboodh. The new integral transform. *Global J. Pure Appl. Math.*, 9(1):35–43, 2013.

[9] M.M. Abdelrahim Mahgoub. The new integral transform mohand transform. *Adv. Theoret. Appl. Math.*, 12(2):113–120, 2017.

[10] M.A. Mahgoub and M. Mohand. The new integral transform "sawi transform". *Adv. Theoret. Appl. Math.*, 14(1):81–87, 2019.

[11] S. Maitama and W. Zhao. New integral transform: Shehu transforma generalization of sumudu and laplace transform for solving differential equations. *Int. J. Anal. Appl.*, 17(2):167–190, 2019.

[12] R. Belgacem, D. Baleanu, and A. Bokhari. Shehu transform and applications to caputo-fractional differential equations. *Int. J. Anal. Appl.*, 17:917–927, 2019.

[13] R. Belgacem, A. Bokhari, and B. Sadaoui. Shehu transform of hilferprabhakar fractional derivatives and applications on some cauchy type problems. *Adv. Theory Nonlinear Anal. Appl.*, 5(2):203–214, 2021.

[14] A. Bokhari, D. Baleanu, and R. Belgacem. Application of shehu transform to atanganabaleanu derivatives. *J. Math. Comput. Sci.*, 20(2):101–107, 2020.

[15] H. Kamal and A. Sedeeg. The new integral transform kamal transform. *Adv. Theoret. Appl. Math.*, 11(4):451–458, 2016.

[16] H. Jafari. A new general integral transform for solving integral equations. *J. Adv. Res.*, 2020.

[17] R. Belgacem, A. Bokhari, D. Baleanu, and S. Djilali. New generalized integral transform via dzherbashiannersesian fractional operator. *IJOCTA*, 14(2):90–98, 2024.

[18] Muhammad Amin S. Murad, Salim S. Mahmood, Homan Emadifar, Wael W. Mohammed, and Karim K. Ahmed. Optical soliton solution for dual-mode time-fractional nonlinear schrödinger equation by generalized exponential rational function method. *Results in Engineering*, 2025.

[19] I. Alraddadi, F. Alsharif, S. Malik, H. Ahmad, T. Radwan, and K.K. Ahmed. Innovative soliton solutions for a (2+1)-dimensional generalized kdv equation using two effective approaches. *AIMS Mathematics*, 9(12):34966–34980, 2024.

[20] P. O. Mohammed, M. R. Alharthi, M. A. Yousif, A. A. Lupas, and S. M. Azzo. Modeling and neural network approximation of asymptotic behavior for delta fractional difference equations with mittag-leffler kernels. *Fractal and Fractional*, 9(7):452, 2025.

[21] Majeed Ahmad Yousif, Dumitru Baleanu, Mohamed Abdelwahed, Shrooq Mohammed Azzo, and Pshtiwan Othman Mohammed. Finite difference β-fractional approach for solving the time-fractional fitzhughnagumo equation. *Alexandria Engineering Journal*, 125:127–132, 2025.

[22] Karim K. Ahmed, Muhammad Bilal, Javed Iqbal, Majeed Ahmad Yousif, Dumitru Baleanu, and Pshtiwan Othman Mohammed. An analytical algebraic method for solving nonlinear fractional differential equations with conformable fractional derivatives. *Contemporary Mathematics*, 6(5):5925–5954, 2025.

[23] I.M. Junaid. The generalization of integral transforms combined with he's polynomial. *Eur. J. Pure Appl. Math.*, 16(2):1024–1046, 2023.

[24] Shengqiang Zhang, Yanling Meng, Amit K. Chakraborty, and Hao Wang. Controlling smoking: A smoking epidemic model with different smoking degrees in deterministic and stochastic environments. *Mathematical Biosciences*, page 109132, 2023.

[25] R. Ullah, M. Khan, and G. Zaman. Dynamical features of a mathematical model on smoking. *J. Appl. Environ. Biol. Sci.*, 6(1):92–96, 2016.

[26] A.A. Kilbas, H.M. Srivastava, and J.J. Trujillo. *Theory and Applications of Fractional Differential Equations*. Elsevier, Amsterdam, 2006.

[27] M. Caputo and M. Fabrizio. A new definition of fractional derivative without singular kernel. *Progress in Fractional Differentiation and Applications*, 73:1–13, 2015.

[28] M. Abdullah, A. Ahmad, N. Raza, M. Farman, and M.O. Ahmad. Approximate solution and analysis of smoking epidemic model with caputo fractional derivatives. *Int. J. Appl. Comput. Math.*, 4:1–16, 2018.

[29] D. Matignon. Stability results for fractional differential equations with applications to control processing. *Comput. Eng. Syst. Appl.*, 2:963, 1996.

[30] C. Li, A. Muhammadhaji, L. Zhang, and Z. Teng. Stability analysis of a fractional-order predatorprey model incorporating a constant prey refuge and feedback control. *Adv. Differ. Equ.*, 2018:325, 2018.